

Phase Diagrams from Topological Transitions: The Hubbard Chain with Correlated Hopping

A. A. Aligia^a, K. Hallberg^a, C. D. Batista^a, and G. Ortiz^b

^aComisión Nacional de Energía Atómica, Centro Atómico Bariloche and Instituto Balseiro,
8400 S.C. de Bariloche, Argentina

^bTheoretical Division, Los Alamos National Laboratory, Los Alamos, NM 87545

(Received August 9, 2021)

The quantum phase diagram of the Hubbard chain with correlated hopping is accurately determined through jumps in π in the charge and spin Berry phases. The nature of each thermodynamic phase, and the existence of charge and spin gaps, is confirmed by calculating correlation functions and other fundamental quantities using numerical methods, and symmetry arguments. Remarkably we find striking similarities between the stable phases for moderate on-site Coulomb repulsion: spin Peierls, spin-density-wave and triplet superconductor, and those measured in (TMTSF)₂X.

The search for electronic mechanisms of superconductivity and the study of superconducting and Mott phase transitions are among the most interesting subjects of the physics of strongly correlated systems. In few cases, exact results have helped to elucidate the nature of these transitions [1–3]. In general one has to rely on numerical calculations of finite systems for which quantities like the Drude weight D_c (which should vanish for an insulator in the thermodynamic limit [4]), or any other correlation function, vary smoothly at the transition. Consequently, for instance, the boundaries between a charge-density-wave (CDW) or spin-density-wave (SDW) insulators and metallic phases in half-filled generalized Hubbard models were difficult to establish [5,6].

The Berry phase is a general geometrical concept which finds realizations in various physical problems [7]. It is the anholonomy associated to the parallel transport of a vector state in a certain parameter space. In condensed matter, the charge Berry phase γ_c is a measure of the macroscopic electric polarization in band or Mott insulators [8] while the spin Berry phase γ_s represents its spin polarization [9,10]. In systems with inversion symmetry γ_c and γ_s can attain only two values: 0 or π (mod 2π). Thus, if two thermodynamic phases differ in the topological vector $\vec{\gamma} = (\gamma_c, \gamma_s)$ this sharp difference allows us to unambiguously identify the transition point even in finite systems. This “order parameter” was recently used to detect metallic, insulator and metal-insulator transitions in one-dimensional lattice fermion models [9,10].

In this Letter we determine the quantum phase diagram of the Hubbard chain with correlated hopping at half-filling using topological transitions. The phase diagram is very rich showing two metallic and two insulating thermodynamic phases each characterized by one of the four possible values of the topological vector $\vec{\gamma}$. One of the metallic phases corresponds to a Tomonaga-Luttinger liquid with dominant triplet superconducting correlations at large distances (TS). This is interesting since there is experimental evidence indicating that the Bechgaard salts (TMTSF)₂ClO₄ and (TMTSF)PF₆ under pressure are TS [11–13]. Furthermore, the insulat-

ing SDW and spin gapped spin-Peierls phase observed in (TMTSF)PF₆ as the pressure is lowered [14] are also present in the model phase diagram.

The effective model Hamiltonian is: [3]

$$H = \sum_{\langle i,j \rangle \sigma} (c_{i\sigma}^\dagger c_{j\sigma} + h.c.) \{t_{AA}(1 - n_{i\bar{\sigma}})(1 - n_{j\bar{\sigma}}) + t_{BB} n_{i\bar{\sigma}} n_{j\bar{\sigma}} + t_{AB} [n_{i\bar{\sigma}}(1 - n_{j\bar{\sigma}}) + n_{j\bar{\sigma}}(1 - n_{i\bar{\sigma}})]\} + U \sum_i (n_{i\uparrow} - \frac{1}{2})(n_{i\downarrow} - \frac{1}{2}). \quad (1)$$

H contains the most general form of hopping term describing the low energy physics of a broad class of system Hamiltonians in which four states per effective site are retained. In particular, the Hamiltonian H in Eq. (1) has been derived and studied for transition metals, organic molecules and compounds [2], intermediate valence systems, cuprates and other superconductors [15]. In the continuum limit, the only relevant interactions at half-filling are U and $t_{AA} + t_{BB} - 2t_{AB}$ [16]. Therefore, we restrict the present study to the electron-hole symmetric case ($t_{AA} = t_{BB} = 1$) which has spin and pseudospin SU(2) symmetries, the latter with generators $\eta^+ = \sum_i (-1)^i c_{i\uparrow}^\dagger c_{i\downarrow}^\dagger$, $\eta^- = (\eta^+)^\dagger$, and $\eta^z = \frac{1}{2} \sum_i (\sum_\sigma n_{i\sigma} - 1)$. The canonical transformation (CT) $\tilde{c}_{i\uparrow} = c_{i\uparrow}$, $\tilde{c}_{i\downarrow} = (-1)^i c_{i\downarrow}^\dagger$ changes the sign of U in H , and interchanges the total spin and pseudospin operators ($\eta^\alpha \longleftrightarrow S^\alpha$). These symmetry properties become crucial in this work. For $t_{AB} = 0$, the model has been solved exactly [3] with the result that the ground state (GS) is highly degenerate. For $t_{AB} \neq 0$ the physics of the model is still unclear and constitutes our main concern.

For the present case $\gamma_{c,s}$ are defined as [9]

$$\gamma_{c,s} = i \int_0^{2\pi} d\phi \langle g_K(\phi, \pm\phi) | \partial_\phi g_K(\phi, \pm\phi) \rangle, \quad (2)$$

where $|g_K(\phi_\uparrow, \phi_\downarrow)\rangle$ is the GS in the subspace with total wave vector K and other quantum numbers kept fixed, with fluxes ϕ_σ for spin σ . Changes in macroscopic polarization with spin σ , P_σ , are related to the corresponding

changes in the Berry phase by: $\Delta P_\uparrow \pm \Delta P_\downarrow = e\Delta\gamma_{c,s}/2\pi \pmod{e}$ [8–10]. Thus, a phase transition will be detected by a jump in π of γ_c (γ_s) if and only if both thermodynamic phases differ in $P_\uparrow + P_\downarrow$ ($P_\uparrow - P_\downarrow$) by $e/2 \pmod{e}$. For example, if one of the phases is a CDW with maximum order parameter (CDWM) and the other a Néel state (N), one is transformed into the other transporting half of the charges (those with a given spin) one lattice parameter. In addition, as explained below, in the present model topological transitions in γ_c and γ_s indicate the opening of the charge and spin gap Δ_c , Δ_s .

We find that the minimum of the GS energy as a function of fluxes, $E_g(\phi_\uparrow, \phi_\downarrow)$, corresponds to the so-called closed shell conditions (CSC): if the number of sites (assumed even) is $L = 2 \pmod{4}$, then $K = \phi_\sigma = 0$, while for L multiple of four $K = \phi_\sigma = \pi$ (which is equivalent to taking antiperiodic boundary conditions and $\bar{K} = 0$ in a system without fluxes).

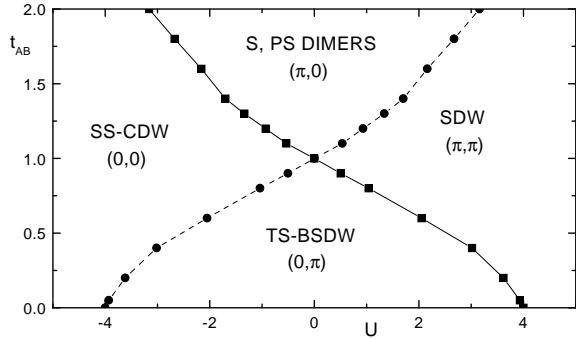


FIG. 1. Quantum phase diagram of the correlated hopping Hubbard chain. The vector Berry phase $\vec{\gamma} = (\gamma_c, \gamma_s)$ and the nature of each stable phase is indicated: Luther-Emery liquid with equally decaying singlet superconductor and CDW correlations (SS-CDW), Tomonaga-Luttinger liquid with triplet superconducting and bond SDW correlations dominating at large distances (TS-BSDW), SDW insulator (SDW), and spin and pseudospin dimerization (S,PS).

For any finite system and fixed t_{AB} , varying U , two topological transitions occur in the model, corresponding to a jump in either γ_c or γ_s . We have determined those transitions in rings of length $L = 6, 8, 10, 12$ using the Lanczos method. The results extrapolated with a cubic polynomial in $1/L$ are represented in Fig. 1. In contrast to other physical quantities which show large finite-size effects, particularly near $t_{AB} = 0$ [6], the topological transitions converge rapidly to the thermodynamic limit (for example, for $t_{AB} = 0.05$, γ_c jumps at $U=3.451, 3.681, 3.788, \text{ and } 3.846$ for $L = 6 - 12$, and the extrapolated value is $U=3.932$). The numerical convergence becomes problematic for smaller t_{AB} values. At $t_{AB} = 0$ the transition points are determined from the exact solution [3] as those values of U where Δ_c and Δ_s

open. Those critical values are $U_{c,s} = \pm 4$ and match smoothly with the rest of the curves in Fig. 1. It is easy to see that under CT the geometrical phases transform as $\gamma_c \longleftrightarrow \gamma_s + \pi$ [9]. Thus, as seen in Fig. 1, a jump in γ_c at U_c (full line) implies a jump in γ_s at $-U_c$ (dashed line), and vice versa.

In the case where all particles are localized one can easily determine the value of $\vec{\gamma}$ as $\gamma_{c,s} = \text{Im} \ln z_L^{c,s}$, where

$$z_L^{c,s} = \langle g | e^{i\frac{2\pi}{L} \sum_j j(n_{j\uparrow} \pm n_{j\downarrow})} | g \rangle, \quad (3)$$

was recently used to study quantum localization [17,18]. In the thermodynamic limit z_L^c vanishes for a conductor while $|z_L^c| \rightarrow 1$ for an insulator. Clearly, $\vec{\gamma}(\text{CDWM}) = (0, 0)$, while $\vec{\gamma}(\text{N}) = (\pi, \pi)$, and by continuity $\vec{\gamma}(\text{CDW}) = (0, 0)$, $\vec{\gamma}(\text{SDW}) = (\pi, \pi)$. On the other hand, it is not easy to predict the values of $\vec{\gamma}$ in conducting phases. However, for $U = 0$, the model is invariant under CT. Therefore $\vec{\gamma} = (\pi, 0)$, or $\vec{\gamma} = (0, \pi)$, indicating a topological difference with the above mentioned CDW and SDW states.

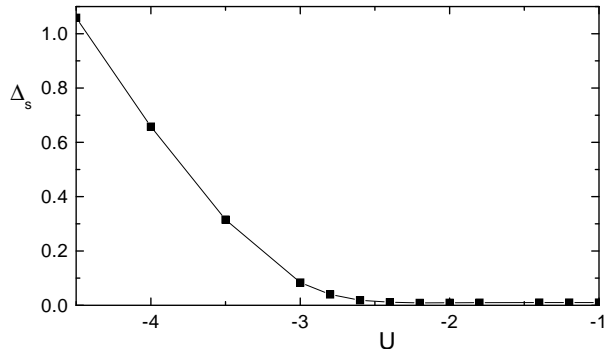


FIG. 2. Spin gap Δ_s as a function of U for $t_{AB} = 0.6$, obtained with DMRG.

Δ_c (Δ_s) vanishes at the left (right) of the full (dashed) line in Fig. 1, and is different from zero at the right (left). It has been shown, that in spin $SU(2)$ symmetric systems the opening of Δ_s can be detected as a level crossing of triplet and singlet states for boundary conditions opposite to the CSC ones (periodic if the number of particles with a given spin N_σ is even, and antiperiodic if N_σ is odd) [19]. It is precisely this crossing which causes the jump in γ_s [10]. A direct evaluation of Δ_s has large finite-size effects, and an accurate calculation requires use of the Density Matrix Renormalization Group (DMRG) method [20]. Fig. 2 displays Δ_s for $t_{AB} = 0.6$ extrapolated from calculations of open chains with length $L \leq 40$. For $-2 < U < -1$, Δ_s vanishes within numerical accuracy (~ 0.01) while for smaller values of U it increases rapidly. These results are consistent with Δ_s opening near $U_s \approx -2.1$ with a singular growth (exponentially small as in the $t - J$ model [19]). The result derived from the topological transition is $U_s = -2.051$.

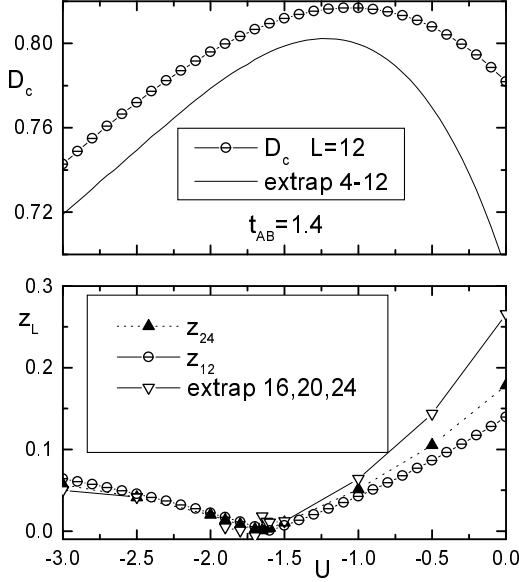


Fig. 3 Aligia

FIG. 3. Drude weight D_c and z_L^c for $t_{AB} = 1.4$ as a function of U for $L = 12$ (open circles) and $L = 24$ (solid triangles). The solid lines are polynomial extrapolations in $1/L$.

The symmetry transformation CT implies that if Δ_s opens at U_s , a pseudospin gap Δ_η opens at $-U_s$. Pseudospin excitations form a subset of all charge excitations. In our case the charge velocity v_c and Δ_c (computed as usual in finite systems $L \leq 12$ [19]) coincide with their pseudospin counterparts v_η and Δ_η (computed from v_s and Δ_s for opposite U) [21]. This is consistent with the exact solution for $t_{AB} = 0$ where the charge excitations of lowest energy are pseudospin ones [3]. In addition, the charge-charge and spin-spin correlation functions are interchanged as U changes sign (see below). The opening of Δ_c where γ_c jumps from 0 to π is also consistent with calculations of z_L^c , D_c , superconducting correlation functions, K_ρ and central charge c . For $t_{AB} > 1$, Δ_c opens more slowly and the detection of the transition becomes more difficult. However, as shown in Fig. 3, D_c and z_L^c display a similar behavior near the jump in γ_c ($U_c = -1.702$) as in the quarter-filled infinite U extended Hubbard model as a function of the nearest-neighbor repulsion V [18], where a metal-insulator transition takes place at $V = 2t$. At large $|U|$ the only relevant energy scale is $4t_{AB}^2/|U|$ and therefore, D_c increases with U for large negative U . Near U_c there is a drastic change of behavior of D_c and z_L^c vs U , and for $U > U_c$, the extrapolated values suggest a tendency to reach the insulating values ($D_c=0$, $z_L^c=1$), in the thermodynamic limit. z_L^c always decreases (increases) with L at the left (right) of U_c . This is the first accurate (DMRG) calculation of z_L^c in a system of more than 16 sites.

In order to further characterize each thermodynamic phase we use symmetry arguments and the following correlation functions (CF) (see Fig. 4):

$$\begin{aligned}
 \chi_{t(s)}(d) &= \frac{1}{2} \langle (c_{0\uparrow}^\dagger c_{1\downarrow}^\dagger \pm c_{0\downarrow}^\dagger c_{1\uparrow}^\dagger) (c_{d+1\downarrow} c_{d\uparrow} \pm c_{d+1\uparrow} c_{d\downarrow}) \rangle \\
 \chi_{os}(d) &= \langle c_{0\uparrow}^\dagger c_{0\downarrow}^\dagger c_{d\downarrow} c_{d\uparrow} \rangle \\
 \chi_c(d) &= -\frac{1}{2} \langle (n_{0\uparrow} + n_{0\downarrow} - 1)(n_{d\uparrow} + n_{d\downarrow} - 1) \rangle \\
 \chi_{bsdw}(d) &= \frac{1}{2} \langle (c_{0\uparrow}^\dagger c_{1\downarrow} + c_{1\uparrow}^\dagger c_{0\downarrow}) (c_{d+1\downarrow} c_{d\uparrow} + c_{d\downarrow}^\dagger c_{d+1\uparrow}) \rangle \\
 \chi_{sz}(d) &= -2 \langle S_0^z S_d^z \rangle, \tag{4}
 \end{aligned}$$

computed with DMRG and CSC [21]. The CF are defined such that, in the non-interacting case, $\lim_{L \rightarrow \infty} \chi(d, L) = 1/(\pi d)^2$, with d an odd number. $\chi_{bsdw}(d)$ corresponds to correlations between spins located in bonds [16]. The GS for CSC is always a spin and pseudospin singlet. Invariance under pseudospin rotations implies that $\chi_{os}(d) = (-1)^{d+1} \chi_c(d)$, i.e. on-site singlet superconducting and charge CF have the same distance dependence. This, in turn, implies $K_\rho = 1$ in the conducting phases [22], meaning that the large distance behavior is dominated by logarithmic corrections. Also, using CT and spin rotations one obtains $\chi_c(d, U) = \chi_{sz}(d, -U)$ and $\chi_t(d, U) = \chi_t(d, -U) = (-1)^d \chi_{bsdw}(d, U)$.

We restrict our study to odd values of d for which the oscillatory factors of the CF in the continuum limit are maximum [22]. In addition we took $L = 2d$, motivated by results on the Heisenberg model [23], showing that $\lim_{L \rightarrow \infty} \chi_{sz}(d, L) = C \chi_{sz}(d, 2d)$, where C is a constant independent of d . This also true, if d is odd, for all CF of our model in the non-interacting case, with $C = (\pi/2)^2$. The above mentioned symmetry relations and analytical results in the non-interacting limit allowed us to check the accuracy of the DMRG results. A summary for each non-equivalent topological region is described below:

- a) $\vec{\gamma} = (\pi, 0), \Delta_c \neq 0, \Delta_s \neq 0$. All CF decay exponentially. To understand the nature of this insulating GS let us analyze the limit $t_{AB} \rightarrow \infty$, where effectively there is a sequence of spin and pseudospin dimers. Each dimer is the ground state of the model for two sites and two particles. Including the dimer-dimer interaction in second-order perturbation theory the resulting GS energy per site is $e \approx -1.0625t_{AB}$ ($e_{\text{DMRG}} = -1.0808t_{AB}$). The energy difference between the two lowest singlet states (with $\vec{K} = 0$ and $\vec{K} = \pi$) decays nearly exponentially with L , indicating a breaking of the translational symmetry in the thermodynamic limit.
- b) $\vec{\gamma} = (\pi, \pi), \Delta_c \neq 0, \Delta_s = 0$. As in the ordinary positive U Hubbard model, the GS is an insulating SDW.
- c) $\vec{\gamma} = (0, 0), \Delta_c = 0, \Delta_s \neq 0$. The system forms a Luther-Emery liquid with χ_s and χ_c CF decaying as $1/d$ (neglecting logarithmic corrections.)
- d) $\vec{\gamma} = (0, \pi), \Delta_c = 0, \Delta_s = 0$. χ_{os} and χ_s display the same long distance behavior (Fig. 4). Because of sym-

metry arguments, for $U = 0$, all CF except $\chi_t = \chi_{bsdw}$ show the same $1/d^2$ decay (apparently without logarithmic corrections). Renormalization group arguments [22] show that when $\Delta_s = 0$, χ_t should decay more slowly than χ_s , and therefore dominate for small $|U|$. As U increases, χ_t decays more rapidly, while the opposite happens with χ_{sz} . Near the opening of Δ_c (at $U_c \approx 2.05$ for $t_{AB} = 0.6$), both CF seem to decay in a similar fashion.

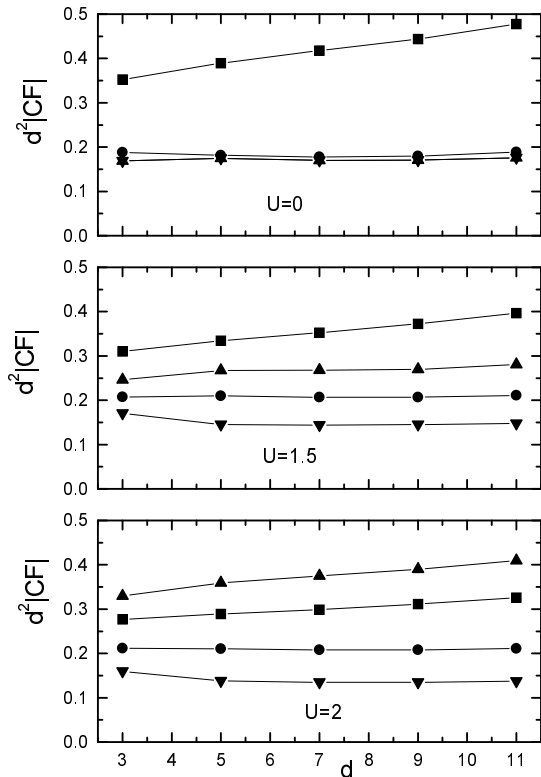


Fig. 4 Aligia

FIG. 4. Correlation functions (CF) times the square of the distance d as a function of d for $t_{AB} = 0.6$: nearest-neighbor triplet $|\chi_t(d)| = |\chi_{bsdw}(d)|$ (squares) and singlet $\chi_s(d)$ (circles) pair CF, on-site pair and charge CF $|\chi_{os}(d)| = |\chi_c(d)|$ (downward triangles), and spin CF $\chi_{sz}(d)$ (upward triangles). See Eq. (4).

In conclusion, we have constructed the quantum phase diagram of Eq. (1) from topological considerations. Each thermodynamic phase is associated to a topological vector, and changes in that quantity signal the transition point. A key finding is the identification of a triplet superconducting phase degenerate with a bond-located SDW for $t_{AB} < 1$ and small $|U|$. Taking into account the slight dimerization in (TMTSF)₂X compounds, an effective Hamiltonian similar to Eq. (1) can be realized, where only four low-energy states per unit cell are kept. Assuming that additional interactions stabilize the TS with respect to the BSDW it is remarkable that, for

$U > 0$, as t_{AB} is decreased a similar sequence of quantum phase transitions takes place as pressure is applied [14]. This general approach can be extended to spatial dimensions higher than one [8], and applied to more general models which do not necessarily have SU(2) pseudospin symmetry [9].

One of us (A.A.A.) thanks J. Voit and L. Arrachea for helpful discussions. We acknowledge computer time at the Max-Planck Institute für Physik Komplexer Systeme. A.A.A., K.H. and C.D.B. are supported by CONICET, Argentina, while G.O. is supported by the US Department of Energy.

-
- [1] B.S. Shastry and B. Sutherland, Phys. Rev. Lett. **65**, 243 (1990); N. Kawakami and S.K. Yang, *ibid* **65**, 3063 (1990); C.A. Stafford and A.J. Millis, Phys. Rev. B **48**, 1409 (1993).
 - [2] R. Strack and D. Vollhardt, Phys. Rev. Lett. **70**, 2637 (1993); references therein.
 - [3] L. Arrachea, A.A. Aligia, and E.R. Gagliano, Phys. Rev. Lett. **76**, 4396 (1996); references therein.
 - [4] W. Kohn, Phys. Rev. **133**, A171 (1964).
 - [5] J.E. Hirsch, Phys. Rev. Lett. **53**, 2327 (1984).
 - [6] L. Arrachea, E.R. Gagliano, and A.A. Aligia, Phys. Rev. B **55**, 1173 (1997).
 - [7] *Geometric Phases in Physics*, edited by A. Shapere and F. Wilczek (World Scientific, Singapore, 1989).
 - [8] G. Ortiz *et al.*, Phys. Rev. B **54**, 13515 (1996).
 - [9] A.A. Aligia and E.R. Gagliano, Physica C **304**, 29 (1998); A.A. Aligia *et al.*, Eur. Phys. J. B **5**, 371 (1998).
 - [10] A.A. Aligia, Europhys. Lett. **45**, 411 (1999).
 - [11] M. Takigawa, H. Yasuoka, and G. Saito, J. Phys. Soc. Jpn. **56**, 873 (1987).
 - [12] I.J. Lee *et al.*, Phys. Rev. Lett. **78**, 3555 (1997).
 - [13] S. Belin and K. Behnia, Phys. Rev. Lett. **79**, 2125 (1997).
 - [14] D. Jérôme, Science **252**, 109 (1991); references therein.
 - [15] M.E. Foglio and L.M. Falicov, Phys. Rev. B **20**, 4554 (1979); H.B. Schüttler and A.J. Fedro, *ibid* **45**, 7588 (1992); M.E. Simon and A.A. Aligia, *ibid* **48**, 7471 (1993); F. Marsiglio and J.E. Hirsch, *ibid* **49**, 1366 (1992).
 - [16] G. Japaridze and A.P. Kampf, cond-mat/9808253.
 - [17] R. Resta and S. Sorella, Phys. Rev. Lett. **82**, 370 (1999).
 - [18] A.A. Aligia and G. Ortiz, Phys. Rev. Lett. (in press).
 - [19] M. Nakamura, K. Nomura, and A. Kitazawa, Phys. Rev. Lett. **79**, 3214 (1997).
 - [20] S. White, Phys. Rev. Lett. **69**, 2863 (1992).
 - [21] For boundary conditions other than open or CSC the DMRG is not accurate enough for our model. Thus, calculations of $\vec{\gamma}$, D_c , $v_{c,s}$, and K_ρ were done using the Lanczos method with $L \leq 12$.
 - [22] J. Voit, Rep. Prog. in Phys. **58**, 977 (1995).
 - [23] K.A. Hallberg, P. Horsch, and G. Martinez, Phys. Rev. B **52**, 719 (1995).